

CrossMark
click for updatesCite this: *RSC Adv.*, 2014, 4, 49995

An integrated process of CO₂ capture and *in situ* hydrogenation to formate using a tunable ethoxyl-functionalized amidine and Rh/bisphosphine system†

Yu-Nong Li, Liang-Nian He,* Xian-Dong Lang, Xiao-Fang Liu and Shuai Zhang

An integrated process of CO₂ capture and *in situ* hydrogenation into formate was achieved in 95–99% yield using a tunable ethoxyl-functionalized amidine and Rh/bisphosphine system, being regarded as an alternative carbon capture and utilization approach to supply fuel-related products, to circumvent the energy penalty in carbon capture and storage. CO₂ was captured by non-volatile amidine derivatives with simultaneous activation to form zwitterionic amidinium carbonate, and subsequent hydrogenation was facilitated by Rh/bisphosphine. The adsorption capacity and hydrogenation efficiency can be optimized by tuning the ethoxyl side chain. Particularly, the alkanolamidine bearing an intramolecular hydrogen donor derived from 1,8-diazabicyclo[5.4.0]undec-7-ene (DBU) gave both a high CO₂ uptake (molar ratio of 0.95 : 1) and excellent hydrogenation yield (99%). Furthermore, the silica-supported alkanolamidine was readily recovered and reused with the retention of good performance. This kind of carbon capture and utilization pathway could be a potential energy-saving option for industrial upgrading of CO₂ from waste to fuel-related products in a carbon neutral manner.

Received 16th August 2014
Accepted 17th September 2014

DOI: 10.1039/c4ra08740b

www.rsc.org/advances

Introduction

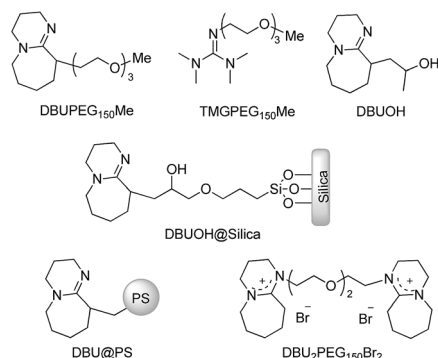
Among numerous schemes to reduce greenhouse gas emissions, carbon capture and storage (CCS) is regarded as one of the most potential measures.¹ However, extensive energy consumption in the desorption/compression process would be a crucial barrier for practical CCS.^{1c} Consequently, carbon capture and utilization (CCU) has been proposed as an alternative approach to circumvent the energy issues in CCS, whereby the captured CO₂ can be used as a non-toxic, abundant, and sustainable feedstock to produce value-added compounds/fuels/materials.² In this context, a high CCU efficiency would offer feasible applications in industry. An elegant combination of CO₂ capture and *in situ* hydrogenation to fuel-related products including formic acid, methanol, and amides, as well as methylated compounds,³ is an appealing strategy to supply renewable energy in a carbon neutral cycle.⁴ In addition, this protocol can avoid high-pressure operations, which are commonly required for hydrogenation reactions involving CO₂.

Formic acid is an extremely attractive liquid hydrogen source and hydrogen carrier for easy storage and transportation.⁵ An organic or inorganic base⁶ is always indispensable to make CO₂ hydrogenation thermodynamically favorable by forming the acid–base adduct.⁷ Furthermore, nonvolatile amino-functional ionic liquids (ILs) and an immobilized base can be applied for this purpose to improve base recovery.⁸ Recently, Hicks *et al.* employed a double-base system consisting of polyethyleneimine (PEI)/Et₃N for CO₂ capture and hydrogenation, respectively. But in this system, the additional base Et₃N was necessary for the hydrogenation.⁹ Base strength and solubility limitations can affect the hydrogenation outcome.¹⁰ In this aspect, amidine compounds have viable basicity and CO₂-affinity, despite few-documented instances.^{10,11} Moreover, based on Jessop's switchable solvent theory,¹² amidine compounds can also be used for CO₂ capture in conjunction with a proton donor to form amidinium carbonate.¹³ In our previous work, *in situ* hydrogenation of the captured CO₂ by PEI and a Rh/monophosphine system was achieved in yield of 37%. Notably, ammonium carbonate exhibited better activity than ammonium carbamate.^{2c} Therefore, it is desirable and assumable to improve catalytic performance for CCU by employing the amidine compound as both the CO₂ absorbent and hydrogenation promoter, which would presumably go through amidinium carbonate hydrogenation.

As expected, CCU efficiency is closely related to both capture capacity and hydrogenation activity. Higher adsorption

State Key Laboratory and Institute of Elemento-Organic Chemistry, Collaborative Innovation Center of Chemical Science and Engineering (Tianjin), Nankai University, Tianjin, 300071, People's Republic of China. E-mail: heln@nankai.edu.cn; Fax: +86-22-2350-3878; Tel: +86-22-2350-3878

† Electronic supplementary information (ESI) available: General experimental methods, experimental procedures and results, characterization for adsorption and hydrogenation systems, and copies of NMR, *in situ* FTIR, FT-IR, GC-MS spectra, TGA and DFT study. See DOI: 10.1039/c4ra08740b



Scheme 1 Amidine derivatives for CO₂ capture and *in situ* hydrogenation.

enthalpy is allowed to attain a larger capacity.¹⁴ Hence, approaches associated with enhancing the basicity *e.g.* introducing an electron-donating substituent have been developed to increase the adsorption capacity.^{14,15} In this respect, amidine compounds can be designed as a base for CO₂ capture due to its high basicity and facile structural modification. More importantly, compared with the published dual-component adsorption systems, amidines with an alkyl chain bearing a hydroxyl group would remove the need of an additional volatile proton donor.¹⁶ An ethoxyl or polyethylene glycol (PEG) substituent could also promote the hydrogenation by adjusting the viscosity and facilitating mass transfer because of their electron-donating, CO₂-philic and thermal-stable properties.¹⁷

We have developed non-volatile amidine derivatives based on the framework of DBU and 1,1,3,3-tetramethylguanidine (TMG) with an ethoxyl-functionalized chain bearing a terminal hydroxyl or methoxy group to tune both CO₂ uptake and hydrogenation activity resulting in remarkably enhanced CCU efficiency. The amidine derivatives in this study are designated as DBUPEG₁₅₀Me, TMGPEG₁₅₀Me, DBUOH, DBUOH@Silica, DBU@PS (PS = Polystyrene), and DBU₂PEG₁₅₀Br₂ as shown in Scheme 1. Herein, the amidine derivatives will serve as a “hinge base” for initial CO₂ capture as an amidinium carbonate species with simultaneous activation and subsequent hydrogenation. This strategy was validated to produce formate in 95–99% yield relative to the captured CO₂ *i.e.* the amidinium carbonate, whose hydrogenation was promoted by RhCl₃·3H₂O/bis(2-diphenylphosphine phenyl)ether (DPEphos) under mild conditions. Especially, a CCU industrial process for CO₂ capture and

in situ hydrogenation along with separation and recycling could be envisioned to avoid desorption, allowing recycling of the absorbent/base as depicted in Fig. 1.

Results and discussion

CO₂ capture

Amidine derivatives were initially studied for CO₂ capture. In this step, protonation occurs presumably at the sp² nitrogen of the amidine derivative, while the ethoxyl-functionalized chain offers additional stabilization for the amidinium cation, facilitating the deprotonated oxygen species to fix CO₂. Remarkably, the enhancement of CO₂-philicity and basicity by the tunable structure of the ethoxyl chain could promote CO₂ sorption with increasing capacity.¹⁸ Generally, more ethoxyl linkages could increase the CO₂-philicity and electron-donating ability, but longer ethoxyl chains may also increase the viscosity.¹⁹ Hence, DBUPEG₁₅₀Me and TMGPEG₁₅₀Me with three C–C–O units, successfully approached equimolar CO₂-capture with a molar ratio of 0.89 : 1 and 1.11 : 1, respectively, owing to their appropriate basicity (entries 1 and 2, Table 1).

In this context, the characteristic signals at 151.29 and 158.73 ppm in the ¹³C NMR spectra support the formation of amidinium alkylcarbonates. The bands centered at 1588, 1405 and 1294 cm⁻¹ in the FT-IR spectra can be assigned to the stretching vibration of the C=O bond of carbonate, basically in agreement with those previously reported^{13c} (see ESI†). But DBU₂PEG₁₅₀Br₂ exhibited no adsorption capacity due to its extremely weak basicity and high viscosity (entry 3). Furthermore, alkanolamidine (DBUOH) with one ethoxyl unit,

Table 1 CO₂ adsorption using amidine derivatives^a

Entry	Absorbent system (mmol mmol ⁻¹)	<i>t</i> (min) ^b	Capacity ^c
1	DBUPEG ₁₅₀ Me/glycol (3/6)	12	0.89
2	TMGPEG ₁₅₀ Me/glycol (3/18)	9	1.11
3	DBU ₂ PEG ₁₅₀ Br ₂ /glycol (3/24)	27	—
4 ^d	DBUOH (3)	9	0.58
5	DBUOH/TGDE (3/5)	27	0.95
6 ^e	DBU@PS/glycol (0.24/24)	18	0.90
7 ^f	DBUOH@Silica/TGDE (0.24/5)	9	3.02
8 ^f	DBUOH@silica/glycol (0.24/24)	15	3.48

^a Amidine derivative (3 mmol), 25 °C. ^b Time required to reach adsorption equilibrium unless otherwise stated. ^c Moles of CO₂ captured per mole of superbase subtracting the solvents physical adsorption. ^d Using DBUOH (3 mmol) without solvent. ^e DBUOH@PS (0.18 g, containing 0.24 mmol DBU) Elemental analysis: N 3.70%, DBU 20.0% in weight. ^f DBUOH@Silica (0.42 g, containing 0.24 mmol DBUOH). Elemental analysis: N 1.60%, DBU 8.69% or DBUOH 11.3% in weight.

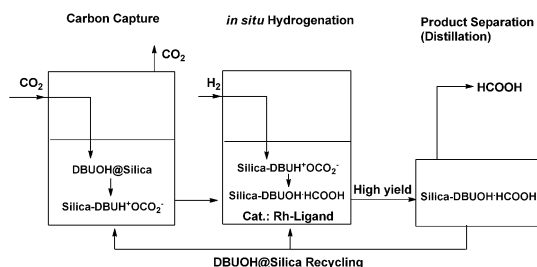


Fig. 1 The hypothetical CCU process proposed in this study.

containing an equal number of amidine and intramolecular hydroxyl groups, can almost capture an equimolar amount of CO₂ in the absence of an additional proton donor (entry 4 and 5). Here, tetraethylene glycol dimethyl ether (TGDE) was used to adjust the viscosity of DBUOH. In the ¹³C NMR spectrum, the additional peak at 164.25 ppm likely corresponds to the intramolecular amidinium carbonate. Besides, the strong band of [C=NH]⁺ at 1646 cm⁻¹, comparable to that of [HDBU]Cl (1645 cm⁻¹),^{12,20} and the peaks corresponding to C=O at 1554, 1421 and 1297 cm⁻¹ can also be observed (see ESI†).

DFT calculated enthalpy changes revealed that the intramolecular carbonate as the adsorption product may undergo a cyclic formation *via* hydrogen bonding (Fig. S1, ESI†). Furthermore, the polystyrene supported DBU/glycol system was able to absorb CO₂ in a molar ratio of 0.90 : 1 (entry 6). Particularly, in the aprotic solvent, TGDE, 0.42 g of DBUOH@Silica (Fig. S4 and S6, ESI†) can absorb 0.73 mmol of CO₂, corresponding to a capacity of 76 mg g⁻¹ gravimetrically. The maximum adsorption ratio can be 3.48 : 1 (88 mg g⁻¹) using DBUOH@Silica in glycol (entries 7 and 8). In the chemisorption process, the maximum adsorption ratio should be around 1.

In addition, DBUOH@silica as a solid absorbent can physically absorb CO₂ besides chemisorption. Thus, the actual adsorption ratio reached more than 1 relative to the effective amount of the 0.24 mmol superbase DBUOH@silica contains. Similarly, the peaks at 1646, 1538, 1456, and 1292 cm⁻¹, and a decrease in the OH signal in the FT-IR spectrum suggest the generation of the amidinium carbonate *via* chemisorption (Fig. 2). In the physical adsorption process, DBUOH@Silica could successfully be utilized for adsorption and desorption measurements (Fig. 3). DBUOH@Silica can physically absorb CO₂ to 6.2 cm³ g⁻¹ (14.2 mg g⁻¹) at 25 °C under 0.12 MPa, which undergoes desorption using a N₂ flow of 0.1 L min⁻¹ (Fig. 3a). Notably, no significant drop in CO₂ adsorption was observed

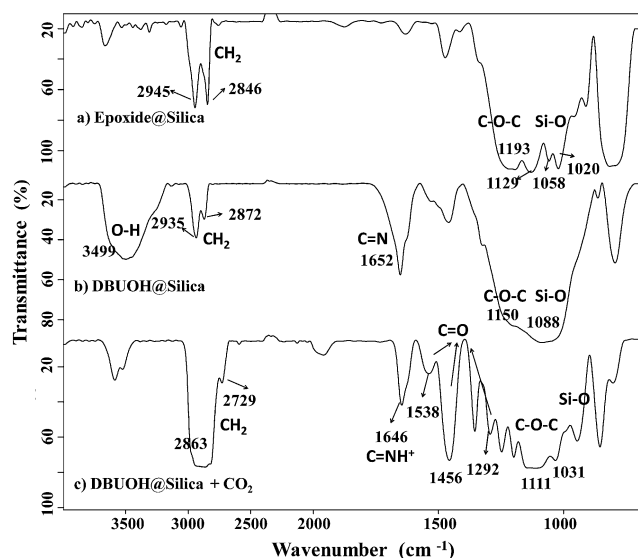


Fig. 2 FT-IR spectra of: (a) Epoxide@Silica; (b) DBUOH@Silica; and (c) DBUOH@Silica + CO₂.

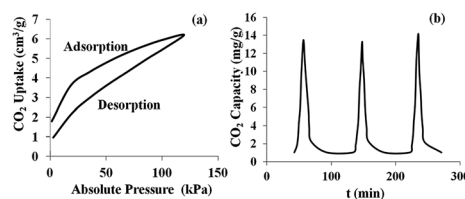


Fig. 3 Reversible CO₂ adsorption and desorption (a) and three consecutive cycles (b) using DBUOH@Silica.

after three successive adsorption-desorption cycles (Fig. 3b), indicating DBUOH@Silica is stable enough to be recycled.

The hydrogenation of gaseous CO₂ to formate

Subsequently, gaseous CO₂ hydrogenation was performed to establish an optimal catalytic system for the *in situ* hydrogenation of the captured CO₂, which is also an activated form of CO₂.

The base effect on the hydrogenation of gaseous CO₂

Considering the promotive effect of bases, amidines were initially compared with a range of organic and inorganic bases for gaseous CO₂ hydrogenation using RhCl₃/PPh₃ at 100 °C. As expected, DBU, TMG, DBN (1,5-diazobicyclo[4.3.0]non-5-ene) and TBD (1,5,7-triazabicyclo[4.4.0]dec-5-ene) showed better activity than conventional amines including TEA (triethanolamine), HMTA (hexamethylenetetramine), Et₃N, Et₂NH, TMEDA (*N,N,N',N'*-tetramethylethylenediamine), DABCO (triethylenediamine), morpholine and DMAP (4-dimethylaminopyridine). Among the amidines used in this study, DBU and TMG displayed superiority with TONs of 362 and 322, respectively (Fig. 4). Although NaOH is a strong base, only a small amount of formate was obtained owing to its solubility limitations and incompatibility with the catalytic system. Moreover, weak bases such as 1-methylimidazole, choline chloride, mono- and di-ethanolamine gave inferior results.

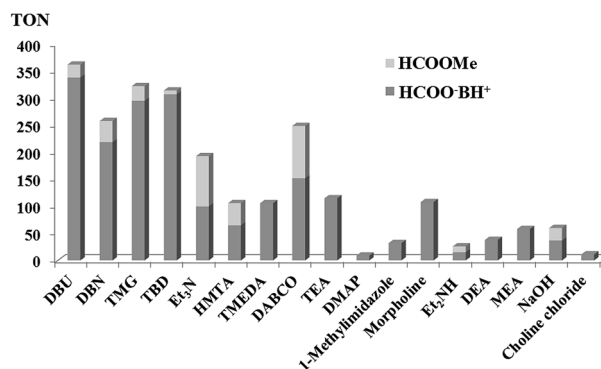


Fig. 4 Comparison of various bases for the hydrogenation of gaseous CO₂ under a pressure of CO₂/H₂ (4/4 MPa) at 100 °C for 16 h. [RhCl₃·3H₂O (0.01 mmol, 2.6 mg), PPh₃ (0.1 mmol, 26 mg), base (3.3 mmol), methanol (3 mL)].

Table 2 Ligand screening for the hydrogenation of gaseous CO₂^a

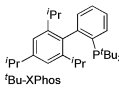
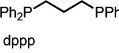
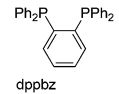
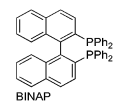
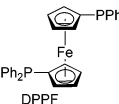
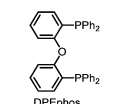
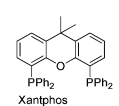
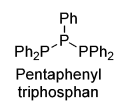
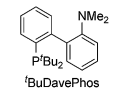
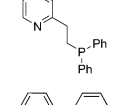
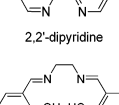
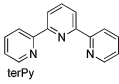
Entry	Ligand	TON ^b
1	—	5
2	PPh ₃	362
3	P ⁿ Bu ₃	290
4	P(2-furyl) ₃	337
5	(<i>o</i> -Tolyl)PPh ₂	441
6	(<i>p</i> -Tolyl)PPh ₂	262
7	CyPPh ₂	480
8	Cy ₂ PPh	473
9		67
10		17
11		69
12		470
13		499
14		516
15		122
16		256
17		249
18		115
19		111
20		46

Table 2 (Contd.)

Entry	Ligand	TON ^b
21		95

^a Reaction conditions: RhCl₃·3H₂O (0.01 mmol, 2.6 mg), monodentate ligand (0.1 mmol) or bidentate/multidentate ligand (0.05 mmol), DBU (3.3 mmol), methanol (3 mL), H₂ (4 MPa), CO₂ (4 MPa), 60 °C, 16 h.
^b Refers to formate including the HCOO⁻BH⁺ adduct and a little HCOOMe calculated by ¹H NMR spectroscopy using 1,1,2,2-tetrachloromethane as an internal standard. TON = turnover number: moles of formate (HCOO⁻BH⁺ and HCOOMe) per mole of Rh catalyst.

Rh/bisphosphine-catalyzed hydrogenation of gaseous CO₂

Screening the phosphine and nitrogen ligands in the catalytic system was further studied as listed in Table 2. CO₂ hydrogenation almost did not occur in the absence of a phosphine ligand (entry 1, Table 2). Obviously, PPh₃ exhibited better activity than PⁿBu₃ and (2-furyl)₃P (entries 2–4). Among the monophosphines derived from PPh₃, the activity increases in the sequence (*p*-tolyl)PPh₂ < PPh₃ < (*o*-tolyl)PPh₂ < Cy₂PPh ≤ CyPPh₂ (entries 2, 5–8), being more or less consistent with nucleophilicity. In contrast, ^tBu-XPhos was decisively inferior presumably due to steric hindrance (entry 9). Moreover, bisphosphines were particularly tested. 1,3-Bis(diphenyl phosphino)propane (dppp) with a flexible chain was proven to be inactive (entry 10). However, when the dppbz, BINAP, dppf and DPEphos ligands were used, the TONs were remarkably improved from 69 to 516, respectively (entries 11–14). This superiority is probably due to the electron-donating ability of their rigid chains compared to dppp, and may also be related to their cone angles when coordinating with the Rh center.²¹ In this regard, DPEphos has supreme merit in view of its large cone angle and strong electron-donating ability that account for the highest activity (entry 14). Though Xantphos' framework is conspicuously similar to DPEphos, it gave a lower formate yield, presumably resulting from unfavorable effects arising from a chelating coordination between its oxygen atom and the metal center (entry 14 vs. 15). Multi-phosphine, P–N ligands, and nitrogen ligands exhibited worse activity in comparison with those bisphosphines (entries 16–21). Hence, ligands with strong electron-donating ability or rigid chains, as well as an appropriate cone angle are favorable for the hydrogenation reaction.

Moreover, Fig. S2 (see ESI[†]) shows that increasing the reaction temperature from 60 to 120 °C caused the product yield to drop sharply, whereas at temperatures below 40 °C it also gave inferior results (Fig. S2a[†]). It is probably because that increasing the temperature is detrimental to the exothermic hydrogenation of CO₂, while lower temperatures may slow down the reaction. As a result, formate with a TON of 1565 can be obtained at the optimal temperature of 60 °C (Fig. S2b[†]). To our delight, a TON

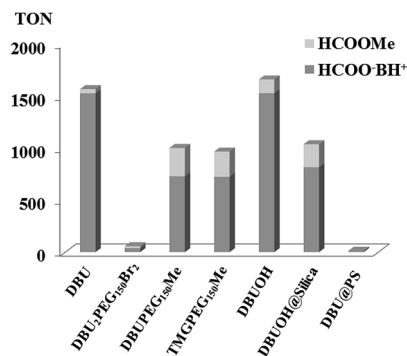


Fig. 5 Amidine derivatives for the hydrogenation of gaseous CO₂. Reaction conditions: RhCl₃·3H₂O (0.01 mmol, 2.6 mg), DPEphos (0.01 mmol, 27 mg), Base (6.6 mmol), methanol (3 mL), CO₂/H₂ (4/4 MPa), 16 h, 60 °C.

of 2202 can be successfully attained through elongating the reaction time to 32 h.

Amidine derivatives as a promoter

With the proper conditions in hand, the modified amidine derivatives were examined for RhCl₃/DPEphos-catalyzed CO₂

hydrogenation in order to further promote the process (Fig. 5). As is well known, the CO₂-philic ethoxyl group could have impacts on the physical properties such as increased gas/liquid diffusion rates, and thus assumedly facilitates the reaction involving CO₂.^{13c} Nevertheless, viscous DBU₂PEG₁₅₀Br₂ as an IL showed too weak basicity to stabilize formic acid, and gave a rather low yield. In order to increase the basicity, the secondary amine *e.g.* TMG was modified to the tertiary amine TMGPEG₁₅₀Me, and DBU was also modified by an electron-donating PEG₁₅₀Me substituent, which could accelerate the formation of HCOOMe. Dramatically, DBUOH as an alkanolamidine performed well with the highest TON of 1698 within 16 h, better than both DBU and DBUPEG₁₅₀Me. The terminal hydroxyl group is assumed to facilitate proton transfer among the reactive species, resulting in the promotion of formate generation,²² albeit its relatively high viscosity. Notably, the silica-supported alkanolamidine (DBUOH@Silica) also exhibited a higher efficiency than the polystyrene supported derivative (DBU@PS).

In situ hydrogenation of the captured CO₂ (CCU)

Hydrogenation of gaseous CO₂ can be efficiently achieved by the tunable ethoxyl-functionalized amidines, which stimulated us

Table 3 Hydrogenation of captured CO₂^a

Entry	Substrate	Adsorption ratio ^d (mol mol ⁻¹)	Captured CO ₂ (mmol)	HCOO ⁻ TON ^b	CCU Yield ^c (%)
1 ^e		0.89 (0.132)	2.77	180	65
2 ^f		1.11 (0.187)	3.59	323	90
3 ^g		0.58 (0.122)	1.74	169	97
4 ^h		0.95 (0.199)	3.02	298	99
5 ⁱ		3.48 (0.088)	1.17	113	96
6 ^j		3.02 (0.076)	0.92	91	99
7 ^k	DBUOH@Silica-CO ₂	2.85 (0.072)	0.88	71	81
8 ^l	DBUOH@Silica-CO ₂	2.37 (0.060)	0.74	66	89

^a Reaction conditions: RhCl₃·3H₂O (0.01 mmol, 1.3 mg), DPEphos (0.05 mmol, 13.5 mg), methanol (2 mL), H₂ (4 MPa), 60 °C, 16 h. ^b Refers to HCOO⁻ BH⁺, determined by ¹H NMR spectroscopy. ^c Relative to the amount of captured CO₂. ^d Moles of CO₂ captured per mole of superbase subtracting solvent physical adsorption. Adsorption ratio (g g⁻¹) is given in brackets. ^e DBUPEG₁₅₀Me (3 mmol)/glycol (6 mmol). ^f TMGPEG₁₅₀Me (3 mmol)/glycol (18 mmol). ^g DBUOH (3 mmol). ^h DBUOH (3 mmol)/TGDE (5 mmol). ⁱ DBUOH@Silica (0.42 g, 0.24 mmol DBUOH)/glycol (24 mmol). ^j DBUOH@Silica (0.42 g, 0.24 mmol)/TGDE (5 mmol). ^k Run 2, DBUOH@Silica (0.42 g)/TGDE (5 mmol). ^l Run 3, DBUOH@Silica (0.40 g, 0.229 mmol DBUOH)/TGDE (5 mmol).

to further investigate the hydrogenation of captured CO₂ by using the amidine derivatives as the “hinge base”, without the addition of extra base. The captured CO₂ *i.e.* amidinium carbonate, could be a simultaneously activated form, which might show higher activity than the gaseous one.

On the basis of the results in Table 1, hydrogenation of those amidinium carbonates formed from CO₂ capture were efficiently performed as summarized in Table 3. TMGPEG₁₅₀Me gave a higher formate yield in regard to captured CO₂ (90%) when compared to DBUPEG₁₅₀Me (65%) due to the higher basicity and lower viscosity of TMGPEG₁₅₀Me (entry 1 vs. 2, Table 3). Dramatically, using DBUOH as the “hinge base”, the formate yield can be improved to 97–99% (entries 3 and 4). On the one hand, DBUOH with a terminal hydroxyl group reached equimolar CO₂ capture, providing enough active CO₂ source for *in situ* hydrogenation. On the other hand, the ethoxyl group could adjust the basicity of the DBU derivatives and the terminal OH could participate in proton transfer during the catalytic cycle. To our delight, the silica-supported DBUOH also worked effectively for *in situ* hydrogenation of captured CO₂ to afford formate in 96–99% yield (entries 5 and 6). As a result, free formic acid can be separated by a filtration and distillation sequence. DBUOH@Silica could be recovered without changing its functionality (Fig. S3, ESI[†]) and was reused for at least three-successive cycles, still giving the desired product in 89% yield after the third run, although its capacity gradually decreased (entries 6–8, Table 3). Significantly, this is an efficient CCU process, removing the energy penalty step, to produce energy-related products from CO₂.

Spectroscopy investigation

Deeper insight into an integration process combining CO₂ capture with *in situ* hydrogenation using a DBUOH/RhCl₃/DPEphos system was investigated by *in situ* FT-IR spectroscopy under CO₂ pressure. In the FT-IR spectrum, the characteristic peak for CO₂²³ at 2340 cm⁻¹ and the appearance of carbonyl peaks at 1271, 1438 and 1577 cm⁻¹ supports the formation of amidinium carbonate upon uptake of CO₂ (Fig. 6), basically consistent with the FT-IR data mentioned above.^{13c} A characteristic peak centered at 1647 cm⁻¹ corresponds to the [C=NH]⁺ band adsorption^{12,20} of protonated DBU. Bands at 1985 and 2006 cm⁻¹, were assigned to the stretching vibration of intermediates with two kinds of Rh–H bonds,²⁴ which gradually increased during the hydrogenation step. The generation of the intermediate formato-Rh complex²⁴ was also observed at 1589 and 1312 cm⁻¹. Broad adsorptions from 1776 to 1805 cm⁻¹ were suggestive of formic acid derivatives.²⁴ The detection of intermediates and products by *in situ* FT-IR spectroscopy would lay a strong foundation for the proposed mechanism.

In addition, the BET (Brunauer–Emmett–Teller) surface area for the solid amidine derivatives *i.e.* DBU@PS and DBUOH@Silica were measured to be 27.3 and 98.5 m² g⁻¹, respectively (Table S1[†]). DBUOH@Silica showed a higher surface area than DBU@PS, and SEM (scanning electron microscopy), also indicated the formation of microparticles on the surface of DBUOH@Silica (Fig. 7). All these physical characteristics could

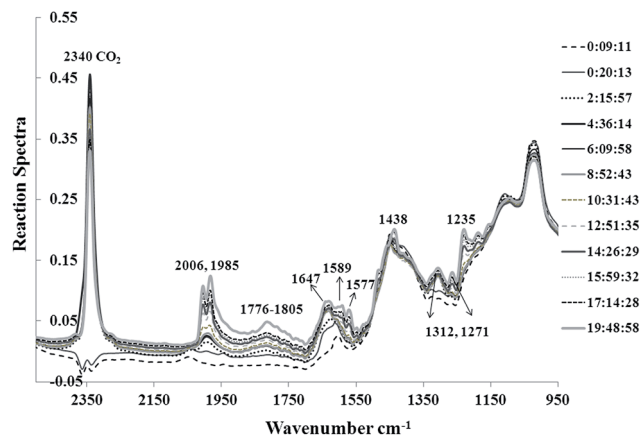


Fig. 6 Monitoring the reaction process by *in situ* FT-IR spectroscopy under CO₂ pressure. Reaction conditions: RhCl₃·3H₂O (0.03 mmol), DPEphos (0.15 mmol), DBUOH (10 mmol), methanol (9 mL), H₂ (4 MPa), CO₂ (4 MPa), 60 °C, 20 h. The spectra of methanol, DPEphos and DBUOH were subtracted.

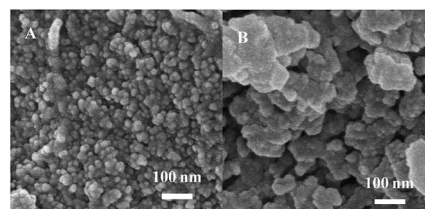
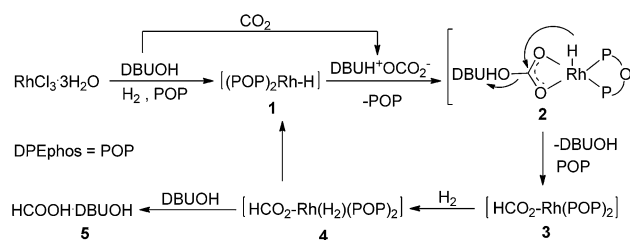


Fig. 7 SEM images of DBUOH@Silica (A) and DBU@PS (B).

promote the interactions between the base and other species, and improve the catalytic efficiency, thus giving higher yields in hydrogenation process.

Reaction mechanism

In spite of the well-documented mechanism on the hydrogenation of gaseous CO₂^{24,25} and CO₂ derivatives,²⁶ a tentative pathway that rationalizes the present process *via* initial CO₂ capture and subsequent hydrogenation to formate is illustrated in Scheme 2. The Rh–H hydride **1** is initially formed from RhCl₃ and DPEphos under H₂ pressure. The CO₂ capture product *i.e.* amidinium alkylcarbonate (DBUH⁺OCO₂⁻) coordinates with the Rh species and thus facilitates intramolecular hydride transfer of **2** and carbonyl insertion into the Rh–H bond, generating the intermediate formato-Rh complex **3**. Subsequently, **4** could be



Scheme 2 The proposed mechanism for CO₂ capture and subsequent Rh-catalyzed hydrogenation of the captured CO₂ using DBUOH.

formed *via* the oxidative addition of H₂, and eventually the reductive elimination of 5 HCOOH·DBUOH occurs, regenerating 1 to complete the catalytic cycle. In this step, DBUOH would participate in the proton transfer, which may not only promote the heterolytic cleavage and δ-bond metathesis of H₂, but also provide protons to 3 in favor of reductive elimination of HCOOH.

Experimental section

Procedure of CO₂ capture

CO₂ capture was carried out in a 10 mL glass tube. The absorbents were charged into the reactor at room temperature. Then, the air in the flask was replaced by CO₂ and a needle used for CO₂ bubbling, which was inserted in the bottom of the glass tube. The adsorption reaction was stirred and conducted with a CO₂ bubbling rate of 0.1 L min⁻¹. The amount of CO₂ absorbed was determined using an analytical balance within an accuracy of ±0.0001 g every three minutes. The measurements of CO₂ sorption by solid absorbent (DBUOH@Silica) were performed on ASAP 2020 Surface Area and Porosity Analyzer (a solid adsorption instrument, which can absorb CO₂ and analyze the change in the amount of physical adsorption as a function of time or pressure). Before measurement, the sample was dried again using the 'outgas' function of the surface area analyzer for about one hour at 50 °C. Adsorption-desorption was determined by several cycles of repeated experiments.

Procedure of gaseous CO₂ hydrogenation

The manipulations were performed in a recirculating mBraun MBio compact inert atmosphere (Ar) drybox at 20 °C. The reaction was carried out in a 50 mL stainless-steel autoclave reactor with an inner glass tube and a magnetic stirrer. Initially, the reaction mixture, consisting of methanol, RhCl₃·3H₂O and the ligand, was transferred to the inner glass and stirred for 10 min. After that, the base was added dropwise to the mixture with stirring. After sealing the autoclave reactor cover, H₂ and CO₂ were introduced to the system with an initial pressure of 4 MPa and 4 MPa, respectively. The reactive mixture was stirred for 16–32 h at 60 °C. After the hydrogenation was complete, the autoclave was cooled to room temperature, and the excess gas depressurized very slowly in ice-water. The resultant mixture was analyzed using NMR spectroscopy with 1,1,2,2-tetrachloromethane as an internal standard. The free formic acid was separated by distillation at 160 °C.

Integrated procedure of CO₂ capture and *in situ* hydrogenation

CO₂ capture was carried out in a 10 mL glass tube. The absorbents were charged into the reactor at room temperature. Then, the air in the flask was replaced by CO₂ and a needle used for CO₂ bubbling, which was inserted in the bottom of the glass tube. The adsorption reaction was stirred and conducted with a CO₂ bubbling rate of 0.1 L min⁻¹. The amount of CO₂ absorbed was determined using an analytical balance within an accuracy of ±0.0001 g every three minutes. Subsequently, the

manipulations were performed under an Ar atmosphere. The CO₂ capture product was dissolved in methanol, then RhCl₃·3H₂O and the ligand were mixed and transferred to the glass tube, which was placed into the 50 mL stainless-steel autoclave. After sealing the autoclave reactor cover, H₂ was led into the system with an initial pressure of 4 MPa. The reactive mixture was stirred for 16 h at 60 °C. The same post-processing and analysis method was used as described above.

Procedure for recycling DBUOH@Silica

After the process of CO₂ capture and *in situ* hydrogenation was completed, the solid was filtrated and washed with methanol, and the formic acid was distilled. The recovered base was a grey powder, which was further dried using a rotary evaporator and at 60 °C under vacuum. The recovered base was directly used for the next run. The reactions were performed under identical reaction conditions described above.

Conclusions

In summary, the efficiency for *in situ* hydrogenation of captured CO₂ has been improved up to more than 99% by employing an ethoxyl-functionalized amidine/Rh/DPEphos sequential system. It is worth mentioning that the ethoxyl linkages could have an electron-donating and CO₂-philic effect that improves the basicity and adjusts the viscosity of the amidine, while the terminal OH group of DBUOH could also lead to desirable proton transfer. Therefore, introducing ethoxyl chains could promote both capture efficiency and hydrogenation activity. This protocol offers a non-volatile, quantitative adsorption with simultaneous activation to form zwitterionic amidinium carbonate, and then *in situ* Rh-bisphosphine-catalyzed hydrogenation of the captured CO₂ can be performed smoothly. Particularly, the recyclable silica-supported alkanolamidine gave high activity without using a volatile proton donor, thereby validating the CCU strategy successfully, which was investigated by NMR and *in situ* FT-IR spectroscopy, as well as TGA, BET, SEM and DFT techniques. This efficient CCU concept could also have the potential practice in industry, circumventing the energy input for the desorption step and generating energy-related products.

Acknowledgements

This work was financially supported by the National Natural Sciences Foundation of China, Specialized Research Fund for the Doctoral Program of Higher Education (20130031110013), and MOE Innovation Team (IRT13022) of China.

References

- 1 For CCS, see: (a) D. M. D'Alessandro, B. Smit and J. R. Long, *Angew. Chem., Int. Ed.*, 2010, **49**, 6058–6082; (b) P. Markewitz, W. Kuckshinrichs, W. Leitner, J. Linsen, P. Zapp, R. Bongartz, A. Schreiber and T. E. Muller, *Energy Environ. Sci.*, 2012, **5**, 7281–7305; (c) M. E. Boot-Handford, J. C. Abanades, E. J. Anthony, M. J. Blunt, S. Brandani,

- N. Mac Dowell, J. R. Fernandez, M.-C. Ferrari, R. Gross, J. P. Hallett, R. S. Haszeldine, P. Heptonstall, A. Lyngfelt, Z. Makuch, E. Mangano, R. T. J. Porter, M. Pourkashanian, G. T. Rochelle, N. Shah, J. G. Yao and P. S. Fennell, *Energy Environ. Sci.*, 2014, 7, 130–189.
- 2 For CCU, see: (a) Z.-Z. Yang, L.-N. He, J. Gao, A.-H. Liu and B. Yu, *Energy Environ. Sci.*, 2012, 5, 6602–6639; (b) A.-H. Liu, R. Ma, C. Song, Z.-Z. Yang, A. Yu, Y. Cai, L.-N. He, Y.-N. Zhao, B. Yu and Q.-W. Song, *Angew. Chem., Int. Ed.*, 2012, 51, 11306–11310; (c) Y.-N. Li, L.-N. He, A. H. Liu, X.-D. Lang, Z.-Z. Yang, B. Yu and C.-R. Luan, *Green Chem.*, 2013, 15, 2825–2829; (d) S. H. Kim, K. H. Kim and S. H. Hong, *Angew. Chem., Int. Ed.*, 2014, 53, 771–774; (e) S. Zhang, Y.-N. Li, Y.-W. Zhang, L.-N. He, B. Yu, Q.-W. Song and X.-D. Lang, *ChemSusChem*, 2014, 7, 1484–1489.
- 3 For fuel-related products of CO₂ hydrogenation, see: (a) Y.-N. Li, R. Ma, L.-N. He and Z.-F. Diao, *Catal. Sci. Technol.*, 2014, 4, 1498–1512; (b) K. Beydoun, T. vom Stein, J. Klankermayer and W. Leitner, *Angew. Chem., Int. Ed.*, 2013, 52, 9554–9557; (c) Y. Li, X. Fang, K. Junge and M. Beller, *Angew. Chem., Int. Ed.*, 2013, 52, 9568–9571; (d) B. Yu, H. Zhang, Y. Zhao, S. Chen, J. Xu, C. Huang and Z. Liu, *Green Chem.*, 2013, 15, 95–99; (e) B. Yu, Y. Zhao, H. Zhang, J. Xu, L. Hao, X. Gao and Z. Liu, *Chem. Commun.*, 2014, 50, 2330–2333; (f) J. H. Kwak, L. Kovarik and J. Szanyi, *ACS Catal.*, 2013, 3, 2094–2100.
- 4 For carbon neutral cycle, see: (a) G. A. Olah, *Angew. Chem., Int. Ed.*, 2013, 52, 104–107; (b) G. A. Olah, A. Goepfert and G. K. S. Prakash, *J. Org. Chem.*, 2009, 74, 487–498; (c) G. A. Olah, *Angew. Chem., Int. Ed.*, 2005, 44, 2636–2639.
- 5 For formic acid as hydrogen carrier, see: (a) H.-L. Jiang, S. K. Singh, J.-M. Yan, X.-B. Zhang and Q. Xu, *ChemSusChem*, 2010, 3, 541–549; (b) S. Enthaler, *ChemSusChem*, 2008, 1, 801–804; (c) J. F. Hull, Y. Himeda, W.-H. Wang, B. Hashiguchi, R. Periana, D. J. Szalda, J. T. Muckerman and E. Fujita, *Nat. Chem.*, 2012, 4, 383–388.
- 6 For base-promoted CO₂ hydrogenation, see: (a) R. Tanaka, M. Yamashita and K. Nozaki, *J. Am. Chem. Soc.*, 2009, 131, 14168–14169; (b) P. G. Jessop, Y. Hsiao, T. Ikariya and R. Noyori, *J. Am. Chem. Soc.*, 1996, 118, 344–355; (c) C. Das Neves Gomes, O. Jacquet, C. Villiers, P. Thuéry, M. Ephritikhine and T. Cantat, *Angew. Chem., Int. Ed.*, 2012, 51, 187–190; (d) H. Hayashi, S. Ogo, T. Abura and S. Fukuzumi, *J. Am. Chem. Soc.*, 2003, 125, 14266–14267; (e) T. J. Schmeier, G. E. Dobereiner, R. H. Crabtree and N. Hazari, *J. Am. Chem. Soc.*, 2011, 133, 9274–9277; (f) Z. Xu, N. D. McNamara, G. T. Neumann, W. F. Schneider and J. C. Hicks, *ChemCatChem*, 2013, 5, 1769–1771; (g) G. A. Filonenko, M. P. Conley, C. Copéret, M. Lutz, E. J. M. Hensen and E. A. Pidko, *ACS Catal.*, 2013, 3, 2522–2526.
- 7 T. Schaub and R. A. Paciello, *Angew. Chem., Int. Ed.*, 2011, 50, 7278–7282.
- 8 (a) S. Wesselbaum, U. Hintermair and W. Leitner, *Angew. Chem., Int. Ed.*, 2012, 51, 8585–8588; (b) Z. Zhang, Y. Xie, W. Li, S. Hu, J. Song, T. Jiang and B. Han, *Angew. Chem., Int. Ed.*, 2008, 47, 1127–1129; (c) Z. Zhang, S. Hu, J. Song, W. Li, G. Yang and B. Han, *ChemSusChem*, 2009, 2, 234–238.
- 9 N. D. McNamara and J. C. Hicks, *ChemSusChem*, 2014, 7, 1114–1124.
- 10 P. Munshi, A. D. Main, J. C. Linehan, C.-C. Tai and P. G. Jessop, *J. Am. Chem. Soc.*, 2002, 124, 7963–7971.
- 11 (a) C.-C. Tai, T. Chang, B. Roller and P. G. Jessop, *Inorg. Chem.*, 2003, 42, 7340–7341; (b) R. J. Perry, T. A. Grocela-Rocha, M. J. O'Brien, S. Genovese, B. R. Wood, L. N. Lewis, H. Lam, G. Soloveichik, M. Rubinsztajn, S. Kniajanski, S. Draper, R. M. Enick, J. K. Johnson, H.-b. Xie and D. Tapriyal, *ChemSusChem*, 2010, 3, 919–930.
- 12 P. G. Jessop, D. J. Heldebrant, X. Li, C. A. Eckert and C. L. Liotta, *Nature*, 2005, 436, 1102.
- 13 For superbases and proton donor systems, see: (a) C. Wang, H. Luo, X. Luo, H. Li and S. Dai, *Green Chem.*, 2010, 12, 2019–2023; (b) C. Wang, H. Luo, D. Jiang, H. Li and S. Dai, *Angew. Chem.*, 2010, 122, 6114–6117; (c) Z.-Z. Yang, L.-N. He, Y.-N. Zhao, B. Li and B. Yu, *Energy Environ. Sci.*, 2011, 4, 3971–3975.
- 14 G. Cui, J. Zheng, X. Luo, W. Lin, F. Ding, H. Li and C. Wang, *Angew. Chem.*, 2013, 125, 10814–10818.
- 15 B. Gurkan, B. F. Goodrich, E. M. Mindrup, L. E. Ficke, M. Massel, S. Seo, T. P. Senftle, H. Wu, M. F. Glaser, J. K. Shah, E. J. Maginn, J. F. Brennecke and W. F. Schneider, *J. Phys. Chem. Lett.*, 2010, 1, 3494–3499.
- 16 (a) M. Kim and J.-W. Park, *Chem. Commun.*, 2010, 46, 2507–2509; (b) P. K. Koech, J. Zhang, I. V. Kutnyakov, L. Cosimbescu, S.-J. Lee, M. E. Bowden, T. D. Smurthwaite and D. J. Heldebrant, *RSC Adv.*, 2013, 3, 566–572.
- 17 (a) D. J. Heldebrant and P. G. Jessop, *J. Am. Chem. Soc.*, 2003, 125, 5600–5601; (b) Y.-N. Li, J.-L. Wang and L.-N. He, *Tetrahedron Lett.*, 2011, 52, 3485–3488.
- 18 Z.-Z. Yang, L.-N. He, Y.-N. Zhao and B. Yu, *Environ. Sci. Technol.*, 2013, 47, 1598–1605.
- 19 Z.-Z. Yang, Q.-W. Song and L.-N. He, *Capture and utilization of carbon dioxide with polyethylene glycol*, Springer, Heidelberg, New York, Dordrecht, London, 2012, p. 78.
- 20 D. J. Heldebrant, P. K. Koech, M. T. C. Ang, C. Liang, J. E. Rainbolt, C. R. Yonker and P. G. Jessop, *Green Chem.*, 2010, 12, 713–721.
- 21 C.-C. Tai, J. Pitts, J. C. Linehan, A. D. Main, P. Munshi and P. G. Jessop, *Inorg. Chem.*, 2002, 41, 1606–1614.
- 22 (a) C. Yin, Z. Xu, S. Yang, S. Ng, K. Wong, Z. Lin and C. Lau, *Organometallics*, 2001, 20, 1216–1222; (b) Y. Himeda, N. Onozawa-Komatsuzaki, H. Sugihara, H. Arakawa and K. Kasuga, *Organometallics*, 2004, 23, 1480–1483.
- 23 E. D. Bates, R. D. Mayton, I. Ntai and J. H. Davis, *J. Am. Chem. Soc.*, 2002, 124, 926–927.
- 24 J. C. Tsai and K. M. Nicholas, *J. Am. Chem. Soc.*, 1992, 114, 5117–5124.
- 25 Y. Musashi and S. Sakaki, *J. Am. Chem. Soc.*, 2002, 124, 7588–7603.
- 26 (a) E. Balaraman, C. Gunanathan, J. Zhang, L. J. W. Shimon and D. Milstein, *Nat. Chem.*, 2011, 3, 609–614; (b) Z. Han, L. Rong, J. Wu, L. Zhang, Z. Wang and K. Ding, *Angew. Chem., Int. Ed.*, 2012, 51, 13041–13045.